

Impedimetric and optical interrogation of single cells in a microfluidic device for real-time viability and chemical response assessment

Conrad D. James^{*}, Nigel Reuel, Eunice S. Lee¹, Rafael V. Davalos, Seethambal S. Mani, Amanda Carroll-Portillo, Roberto Rebeil, Anthony Martino, Christopher A. Apblett

Sandia National Laboratories, PO Box 5800, Albuquerque, MS 87185-1080, United States

Received 22 May 2007; received in revised form 6 August 2007; accepted 31 August 2007

Available online 6 September 2007

Abstract

We report here a non-invasive, reversible method for interrogating single cells in a microfluidic flow-through system. Impedance spectroscopy of cells held at a micron-sized pore under negative pressure is demonstrated and used to determine the presence and viability of the captured cell. The cell capture pore is optimized for electrical response and mechanical interfacing to a cell using a deposited layer of parylene. Changes in the mechanical interface between the cell and the chip due to chemical exposure or environmental changes can also be assessed. Here, we monitored the change in adhesion/spreading of RAW264.7 macrophages in response to the immune stimulant lipopolysaccharide (LPS). This method enables selective, reversible, and quantitative long-term impedance measurements on single cells. The fully sealed electrofluidic assembly is compatible with long-term cell culturing, and could be modified to incorporate single cell lysis and subsequent intracellular separation and analysis.

© 2007 Elsevier B.V. All rights reserved.

Keywords: Impedance spectroscopy; Single cell; Microfluidics; Microfabrication; Macrophage; Immune response

1. Introduction

Microfluidic systems are currently being developed for interrogating living cells in nanoliter-volume microenvironments with precise dosing of chemical reagents. Single cells and large cell networks are of interest, and specifically, researchers are monitoring the response of living cells to various “challenges” (soluble and adsorbed molecules, electric fields, changes in temperature, pH, etc.) for both short and long-term periods (Whitesides et al., 2001; Li et al., 2003). Investigators are pursuing minimally invasive microsystems that provide long-term housing for cell culture, cell manipulation, and optical and/or electrical analysis of cells and cell secretions (Thompson et al., 2004; Davidsson et al., 2004; Shackman et al., 2005; Munoz-Pinedo et al., 2005). Other labs have developed more invasive systems that are capable of lysing cells immobilized on microfabricated obstructions (Di Carlo et al., 2005; Valero et al., 2005) and subsequent DNA extraction and quantitative anal-

ysis (Lee—Lab on a Chip, 2006). Most of these systems rely on optical monitoring of fluorophores for long-term studies, and the drawbacks of such optically based methods include photobleaching, low signal-to-noise ratios, and complex off-chip fluorophore-incorporation procedures. Also, no currently existing microsystems are capable of both non-invasive long-term monitoring of living cells, followed by selective intracellular interrogation and quantitative analysis at the level of single cells. Typically, small populations of immobilized cells are pooled and analyzed, but this can obscure dynamic information at the level of single cells and lead to a misinterpretation of data (Lidstrom and Meldrum, 2003; Longo and Hasty, 2006; Di Carlo and Lee, 2006). A significant step forward in microsystem-enabled biology would be provided by a system that bridges the gap between quasi-bulk population measurements and quantitative single cell analysis. Such a system could be used to investigate the importance of single-cell heterogeneity in quasi-bulk data taken in conventional microchamber studies (Thompson et al., 2004; Davidsson et al., 2004; Wieder et al., 2005).

As mentioned earlier, optical detection methods are often used to monitor living cells, however alternating current (ac) impedance spectroscopic methods provide several advantages for long-term monitoring of living cells (Giaever and Keese,

^{*} Corresponding author. Tel.: +1 505 284 9546; fax: +1 505 844 2991.

E-mail address: cdjame@sandia.gov (C.D. James).

¹ Now at the University of California at Berkeley.

1991). Impedimetric monitoring is non-invasive when using higher frequencies and low amplitude probing signals. This obviates the need for complex fluorescent staining or reporter construct methods typically required for optical detection, and also avoids the difficulties that arise from photobleaching. Impedimetric monitoring systems can utilize bulk electrodes or large surface-area thin film electrodes in order to minimize electrode polarization and electrolysis effects. Such systems have been used for real-time long-term monitoring of cell spreading/adherence/motility in response to adsorbed or soluble chemicals (Kowolenko et al., 1990; Keese and Giaever, 1994; Wegener et al., 2000). Recently, several labs have developed impedance spectroscopy methods for single cells using micro-holes for capturing cells under negative pressure (Huang et al., 2003; Han and Frazier, 2006; Cho and Thielecke, 2007). Bulk or thin-film electrodes are then used to measure the impedance across the micro-hole. However, these measurements were short-term (<10 min) and utilized either rigid or thick membranes for the micro-hole, a configuration that can induce damage to captured cells. Similar cell-capture configurations have been utilized to perform patch clamp measurements (Fertig et al., 2002; Klemic et al., 2005; Pantoja et al., 2004; Matthews and Judy, 2006) as well as single cell electroporation and lysis (Lee—Bioelectrochemistry, 2006).

Here we demonstrate a microelectrofluidic system for capturing single cells and optically and electrically interrogating the cells for extended time periods (~2 h). Single cells are impedimetrically monitored in real-time at a specific excitation frequency for the duration of an experiment. Also, a frequency spectrum (1–10⁵ Hz) of the captured cell is taken at different time-points to provide deeper insight into the cell–chip coupling. The cell capture chips utilize a simple fabrication process flow to create small micron-sized capture pores for applying vacuum to reversibly capture single cells. The chip is coated with Parylene C, a flexible biocompatible polymer, to provide improved electrical insulation, and to provide a flexible mechanical interface for the cell that reduces cell adhesion and damage to the cell membrane during capture. The system is capable of single cell capture with optical and impedimetric confirmation. Cells are then assessed for viability by rapidly analyzing the impedance across the captured cell. The format permits continuous perfusion of culture media and chemicals for assessing long-term responses of cells to particular challenges. Here, our model system consists of RAW264.7 murine macrophages exposed to lipopolysaccharide (LPS), a purified component of Gram-negative bacteria that elicits an immune response in macrophages.

2. Materials and methods

2.1. Device fabrication

Capture pore chips are fabricated on 6 in. (100) 0.675 mm thick silicon wafers (Fig. 1a). Wafers are coated with a 1- μ m thick low-stress silicon nitride film and then the nitride is patterned with reactive-ion etching on the front side to define capture pores with a diameter of 3 or 6 μ m. The backside of

the wafer is patterned to define the mask for bulk silicon etching in KOH (85 °C). Backside ports are 1 or 2 mm wide, yielding 65 μ m or 1 mm wide nitride membranes on the front side of the wafer, respectively. To prepare for parylene deposition, chips are coated with an adhesion promoter, 1% 3-(trimethoxysilyl)propyl methacrylate in a 25/75 water/isopropanol mixture. Acetic acid was added to the adhesion promoter to adjust the pH to 4–5. After soaking chips in the adhesion promoter for 20 min, the chips are rinsed in water and dried. Chips are then coated (PDS2010, Specialty Coating Systems Inc.) with 1.25 μ m of Parylene C using a timed physical vapor deposition (deposition rate ~5 μ m/h). Parylene C has been shown to be biocompatible, and is highly resistant to water absorption, electrical noise, and dielectric breakdown in comparison to many polymers (Suzuki et al., 2004; Feili et al., 2005). Capture pores are then profiled with scanning electron microscopy (SEM) and atomic force microscopy (AFM). Fig. 1b shows an SEM image of a coated capture pore. A slight contrast difference (arrow) indicates the region where the original silicon nitride edge is located as confirmed by AFM measurement of an uncoated pore diameter (3.8 μ m). The AFM linescan in the inset of Fig. 1b shows a more beveled edge at the capture pore compared to the sharp interface of the uncoated capture pore linescan (not shown). Fig. 1c shows a cross-section schematic of the parylene coated capture pore based on AFM and SEM imaging. The inner diameter of the pore is reduced from 3.8 to 1.1 μ m, and the sharp nitride edge is slightly beveled by the parylene layer.

2.2. Cell capture pore model circuit

The capture pore can be modeled as a parallel RC circuit, with a resistance (R_p) through the pore and a capacitance (C_p) across the nitride/parylene membrane. An additional resistance R_b can be added in series to the circuit on both sides to account for the bulk resistance of the fluid on either side of the chip. When modeled in this fashion, the complex impedance of the pore is given by:

$$Z_p = \text{Re}\{Z_p\} + j \text{Im}\{Z_p\} = \frac{R_p}{1 + (\omega R_p C_p)^2} - j \frac{\omega R_p^2 C_p}{1 + (\omega R_p C_p)^2} \quad (1)$$

This can also be represented as the impedance magnitude and phase:

$$|Z_p| = \frac{R_p}{\sqrt{1 + (\omega R_p C_p)^2}}, \quad \angle Z_p^{\circ} = -\tan^{-1}(\omega R_p C_p) \quad (2)$$

At low frequencies, a pure resistance through the pore will have $\angle Z_p^{\circ}$ approaching 0°, while a pure capacitance across the pore will have a $\angle Z_p^{\circ}$ approaching 90°. The value for C_p is largely given by the footprint of liquid in contact with the chip and can be controlled by the chip packaging. When a cell is pulled down to the capture pore under negative pressure, the cell blocks the conductive path through the chip, leading to an increase in resistance across the capture pore. The presence of the cell at the pore places a large resistance (through the cell–chip interface) in series with the original R_p (Cho and Thielecke, 2007). The measured capacitance across the chip will largely be

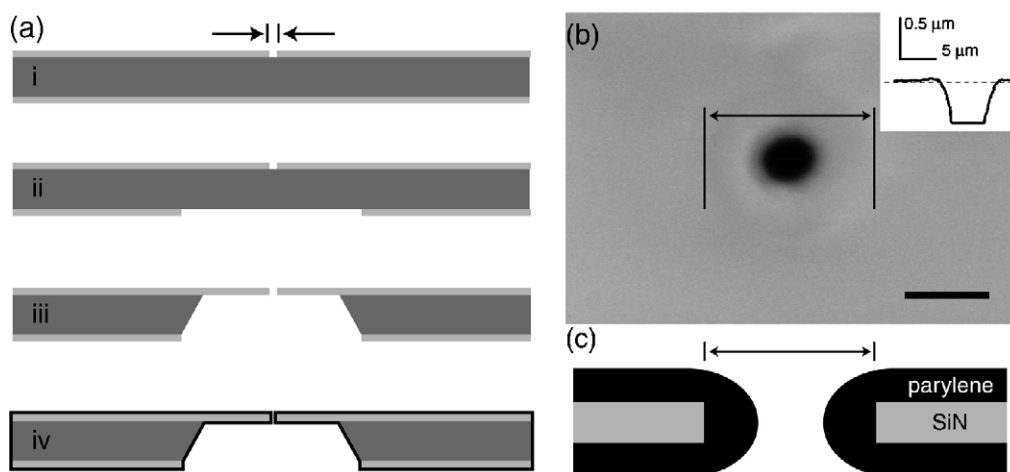


Fig. 1. (a) Fabrication of the single cell capture pore chip. The capture pore is etched in the front-side low-stress nitride (i), followed by an etch of the backside ports (ii). KOH etching is performed, leaving a nitride membrane (iii), followed by a parylene deposition (iv). (b) SEM of a capture pore coated with parylene. Scale bar = 2 μm. (Inset) An AFM linescan of the pore. (c) Cross-section schematic of a capture pore coated with parylene.

unchanged by the presence of the cell unless C_p is on the order of the capacitance of a single cell (~ 1 pF).

2.3. Experimental setup

The electrofluidic packaging for the chips was designed to be modular and reconfigurable in order to simplify assembly and re-use. There is an isolated fluid volume on either side of the chip and connected only through the capture pore. This will confine the electric field lines to pass through the capture pore, enabling impedimetric monitoring of a single cell held at the capture pore. This configuration will also permit single cell lysis with a large amplitude dc electric field.

2.3.1. Electrofluidic assembly

Fig. 2a shows the electrofluidic assembly for impedimetric testing of the chips (Lee—Bioelectrochemistry, 2006). The package consists of a top fluid chamber and a duplicate bottom fluid chamber (machined out of acrylic) separated by the chip. A single silver–silver chloride electrode (In Vivo Metric, Healdsburg, CA) is inserted on each side for two-electrode measurements. Each side also contains a fluidic inlet and outlet interfaced with PEEK microfluidic fittings that connect to 350 μm O.D. silica capillaries (Labsmith Inc., Livermore, CA). Each side of the assembly has a coverslip interface for optical inspection of cells captured at the chip. The top and bottom chambers are interfaced to each side of the chip using a PDMS gasket. The PDMS gasket was made using the following procedure: inlets and outlets were plugged with sacrificial capillaries and held in place with fittings. Each fluid chamber was slightly over-filled with uncured polydimethylsiloxane (PDMS) so that the PDMS bulges slightly above the height of each chamber. After curing, the sacrificial capillaries are removed, leaving fluid channels behind in the PDMS. Cell chambers were then manually cut out of the PDMS gaskets using a razor blade, while ensuring the capillary-made fluid channels interface to the chambers. The bulging PDMS gaskets then seal to the silicon chip when the chambers are assembled together. The native assem-

bly has approximately 200 μL of volume on each side, yielding a fluidic footprint on either side of the chip of $\sim 300 \mu\text{m}^2$. The large fluidic volumes of the chambers reduce the damaging shear effects on captured cells (Walker et al., 2004). With the PDMS gasketing, the volumes on either side can be reduced to 50 μL. The fully assembled package is shown in Fig. 2b. After assembling the electrofluidic package, the bottom chamber is filled with liquid media through the bottom inlet until fluid exits the bottom outlet. The outlet is then closed, and pressure is applied to the bottom inlet to force liquid through the capture pore. After liquid is observed flowing through the capture pore, the top chamber is filled through the inlet until fluid exits the outlet.

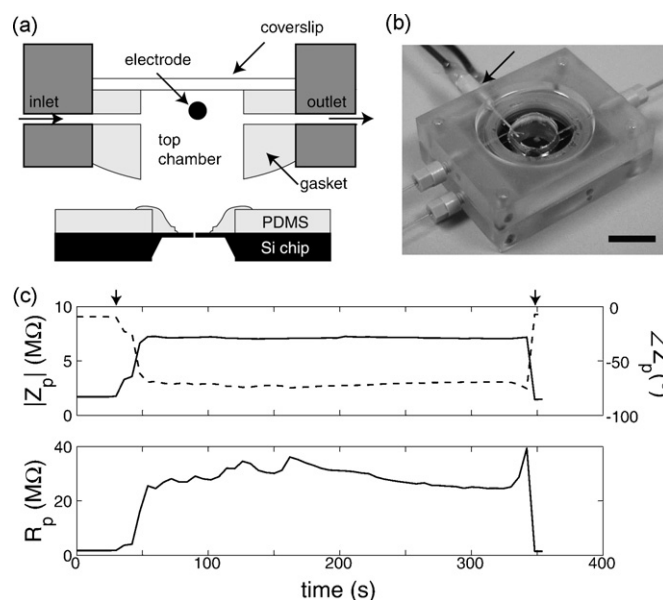


Fig. 2. (a) Schematic of the electrofluidic assembly for impedimetric monitoring of single cells. The bottom chamber is a duplicate of the top chamber. (b) Image of the electrofluidic assembly with coupled electrodes (arrow). Scale bar = 10 mm. (c) Time sweep of $|Z_p|$ (solid line) and Z_p^0 (dashed line) at $f=100$ Hz during the capture (first arrow) and release (second arrow) of a single macrophage. The calculated value of R_p during this experiment is plotted below.

2.3.2. Impedance measurements

Impedance measurements are performed with a PC4/FAS1 potentiostat (Gamry Instruments Inc., Warminster, PA) using a 50 mV voltage amplitude and frequencies from 1 to 10^5 Hz. Single frequency time sweeps were performed with a sampling rate of one measurement every 6 s to measure the complex impedance of the capture pore as a function of time. Data was smoothed with a five-point moving average. Frequency sweeps were taken with five sample points per frequency decade. Raw impedance magnitude and phase data were then fit for values of R_p and C_p using Eq. (2).

2.3.3. Device and assembly optimization

The electrofluidic package was optimized to increase the sensitivity of the system to impedimetric changes in captured cells in response to various challenges. For interrogating captured cells, reducing C_p will enable the detection of changes in the cell membrane capacitance, while increasing R_p will improve sensitivity to changes in the mechanical seal between the cell and the chip. The parylene coating provides three advantages in this regard: (1) the coating reduces the capacitance across the chip by increasing the membrane thickness (which is inversely proportional to C_p), and due to the lower dielectric constant (proportional to C_p) of parylene (~ 3 for parylene and 7 for nitride); (2) the coating insulates bare silicon on the backside of the chip (made during the KOH etch) that is exposed to fluid during an experiment, thus reducing the total capacitance from the backside to the frontside of the chip; and (3) the deposited parylene reduces the capture pore diameter, thus increasing R_p and the resistance through the seal between the cell and the capture pore. The parylene layer also smoothes the sharp edges of the etched pore, providing an interface that will minimize damage to cells during capture. Chips with and without parylene were impedimetrically measured using the frequency sweep method. Chips without parylene typically had C_p values of ~ 7 nF, while a 1.25 μm thick parylene coating reduced C_p to ~ 1.2 nF (Supplementary figure). Chip capacitance was further reduced by placing a thin membrane (300 μm thick) of cured polydimethylsiloxane (PDMS) on top of the chip (Fig. 2a). The PDMS membrane has an opening in the center to maintain the opened capture pore. Medical-grade silicone (MED-1524, NuSil Technology) was then manually applied to the PDMS membrane–nitride chip interface using a steel probe tip (Fig. 2a). The silicone was painted into the near vicinity of the capture pore and cured at 60 °C on a hotplate. Using this method, chip capacitances are reduced to ~ 100 pF, with a minimum attained C_p of 14 pF.

2.3.4. Cell preparation

RAW 264.7 (ATCC) cells were grown to semi-confluency in growth medium [DMEM (ATCC) supplemented with 10% FBS and 5% penicillin–streptomycin] in 5% CO_2 at 37 °C. For cell retrieval, spent media was removed and cell monolayers were briefly washed with Phosphate Buffered Saline (Cellgro). Trypsin–EDTA was added in a volume which sufficiently covered the monolayer, and flasks were incubated briefly at 37 °C to allow for cells to detach. Growth medium was added to

trypsinized cells, and flask walls were washed with growth medium to ensure collection of all cells. Cells were then pelleted at $400 \times g$ for 5 min at room temperature. The cell pellet was resuspended in Trypan Blue (Sigma–Aldrich) and then brought up to a 1 mL volume with growth medium. Cell counts were performed using a hemacytometer, and the final volume of growth media added was adjusted to generate $1\text{--}2 \times 10^6$ cells/mL. Cells were maintained in a 15 mL conical at 37 °C, 5% CO_2 until use. For experiments involving challenge with LPS, growth medium containing 100 $\mu\text{g}/\text{mL}$ of purified *Escherichia coli* LPS (Sigma) was equilibrated to 37 °C, 5% CO_2 .

3. Experimental results

3.1. Impedimetric monitoring of single cells

Impedimetric monitoring provides a non-invasive method to: (1) detect the presence of a cell, (2) assess the viability of the cell, and (3) monitor changes in the cell–chip interface in response to chemical challenges to the cell. The use of suction at a capture pore renders the analysis procedure reversible, enabling selective interrogation of cells based on impedimetric characteristics.

3.1.1. Detection of cell capture

For experiments involving macrophages, the electrofluidic assembly was filled with warmed and gas-equilibrated growth medium prior to injection of cells. Once filled, a syringe pump (Hamilton Scientific) was used to flush the top chamber with growth medium at 100 $\mu\text{L}/\text{min}$ for 10 min. An external three-way luer-lock valve was then used to switch from growth medium to cells suspended in growth medium. Cells were injected into the top chamber at 100 $\mu\text{L}/\text{min}$ to minimize transit time. Once cells were visualized in the top chamber, the flow rate was reduced to 20 $\mu\text{L}/\text{min}$. At this flow-rate, the top chamber is replenished every 2–10 min. For time-course measurements, we monitor the impedance magnitude and phase to readily ascertain the resistive or capacitive nature of the pore. The impedance of the empty pore is taken as a baseline measurement. Negative pressure is then manually applied to the syringe connected to the capture pore (for ~ 10 s at 5–10 psi below atmosphere), and after the negative pressure is slowly released, the cell remains held at the pore. After the cell is held stable for several minutes, the three-way valve is switched back to infusing growth medium at 20 $\mu\text{L}/\text{min}$. Fig. 2c shows the capture of a single macrophage at a chip while measuring the complex impedance of the pore at 100 Hz as a function of time. The raw $|Z_p|$ and $\angle Z_p^0$ are shown at the top, along with the calculated value of R_p (fit according to Eq. (2)) at the bottom. The first arrow indicates when the cell is captured after negative pressure is applied to the bottom chamber at $t = 36$ s. The cell is released by applying positive pressure at $t = 348$ s. When the cell is captured, R_p increases from 1.8 ± 0.03 to 27 ± 6 M Ω . After the cell is released, the R_p returns to 1.5 ± 0.007 M Ω . Application of positive pressure is used to remove the cell and a return to the baseline impedance indicates the pore is free from cell debris. Non-cellular particulates are easily distinguished from cells in this device. Tests with 8 μm diameter latex beads showed much lower increases

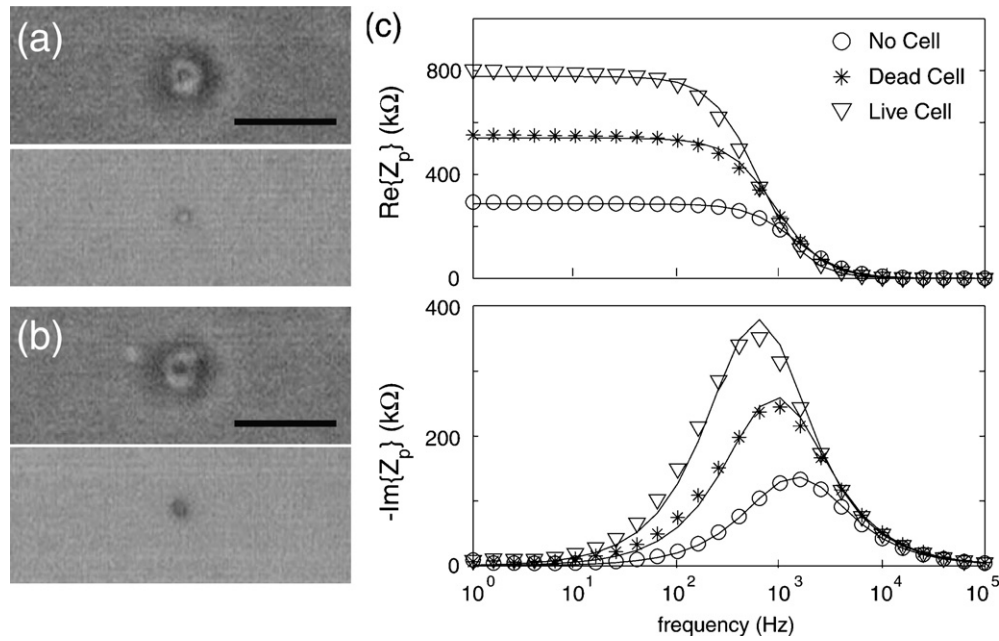


Fig. 3. (a) Image of a captured live cell in phase-contrast (top) and the corresponding brightfield image (bottom). (b) Image of a captured dead cell in phase-contrast (top) and the corresponding brightfield image (bottom). Scale bars = 20 μ m. (c) Averaged real and imaginary components of Z_p for the no cell ($n=6$; fit with $R_p = 286 \pm 34$ k Ω , $C_p = 409 \pm 140$ pF; $r^2 = 0.9994$), dead cell ($n=12$; $R_p = 539 \pm 158$ k Ω , $C_p = 308 \pm 10$ pF; $r^2 = 0.9985$), and live cell ($n=5$; $R_p = 788 \pm 230$ k Ω , $C_p = 328 \pm 10$ pF; $r^2 = 0.9978$) states of the capture pore.

in R_p after capture, due to the inability of rigid particulates to conform to the contour of the capture pore and form a tight seal.

3.1.2. Live/dead discrimination

We utilized a trypan blue stain to validate the impedimetrically determined viability of captured macrophages. Cells with damaged membranes uptake the chromophore, while live cells remain unstained. The depth of fluid through which captured cells are imaged is ~ 1 mm, leading to reduced contrast of the trypan blue stain. Fig. 3ab shows an example of phase contrast and brightfield images of a live cell and a dead cell held at the capture pore. Fig. 3c shows the real ($Re\{Z_p\}$) and imaginary ($Im\{Z_p\}$) components of Z_p as a function of frequency for three states of the pore: no cell ($n=6$), a dead cell ($n=12$), or a live cell ($n=5$). Data points are the mean data points of each state, and solid lines are RC fits to the means. The data was taken in the same experiment using the same chip and batch of macrophages. Fig. 4 shows the complex impedance plot of the $Re\{Z_p\}$ versus $Im\{Z_p\}$. The simple semicircle curves are indicative of a single time-constant parallel RC system. The low-frequency behavior of $Re\{Z_p\}$ and the mid-frequency behavior of $Im\{Z_p\}$ can be used to characterize the viability of captured cells. The means of $Re\{Z_p(1 \text{ Hz})\}$ for each of the three states was 294 ± 34 k Ω (empty), 552 ± 160 k Ω (dead), and 816 ± 240 k Ω (live), with a significance of the mean variances of $p < 1.4 \times 10^{-4}$ (one-way ANOVA). The means of $Im\{Z_p(1000 \text{ Hz})\}$ for each of the three states was -128 ± 17 k Ω (empty), -245 ± 69 k Ω (dead), and -316 ± 46 k Ω (live), with a significance of the mean variances of $p < 0.62 \times 10^{-4}$ (one-way ANOVA). Thus, for a given experiment, the values of $Re\{Z_p(1 \text{ Hz})\}$ and $Im\{Z_p(1000 \text{ Hz})\}$ for the empty state of the pore can be taken, and by thresholding those values appropriately (in this case by $\sim 3\times$), we can exclude a

large percentage of non-cellular particulates (see Section 3.1.1) and dead cells, and ensure a more homogeneous population of live cells for subsequent chemical challenge.

3.1.3. Chemical challenge

Macrophage spreading/adherence has been a topic of interest for many years due to the role of macrophages in the innate immune response (Rabinovitch and Destefano, 1974; Morland and Kaplan, 1977). Immune stimulants such as LPS promote increased spreading and attachment of macrophages in vitro. Upon binding to the cell membrane of macrophages, LPS triggers a signaling cascade that leads to increased $\beta 2$ -integrin function and increased integrin-dependent adhesion and spread-

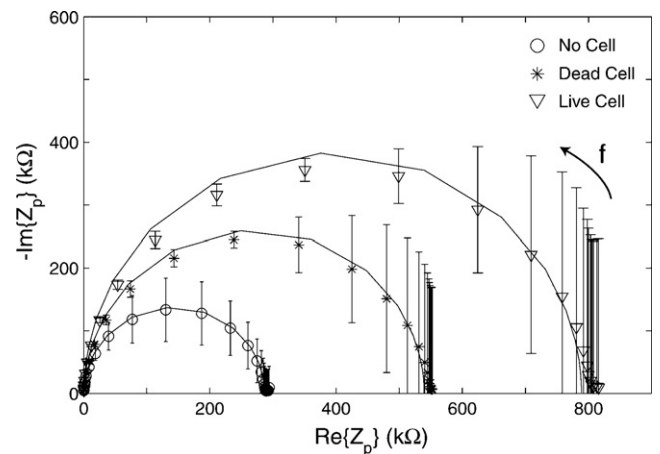


Fig. 4. Complex plane impedance plot of the three pore states from Fig. 3. Solid lines are RC element fits to the experimental data. The direction of increasing frequency is indicated.

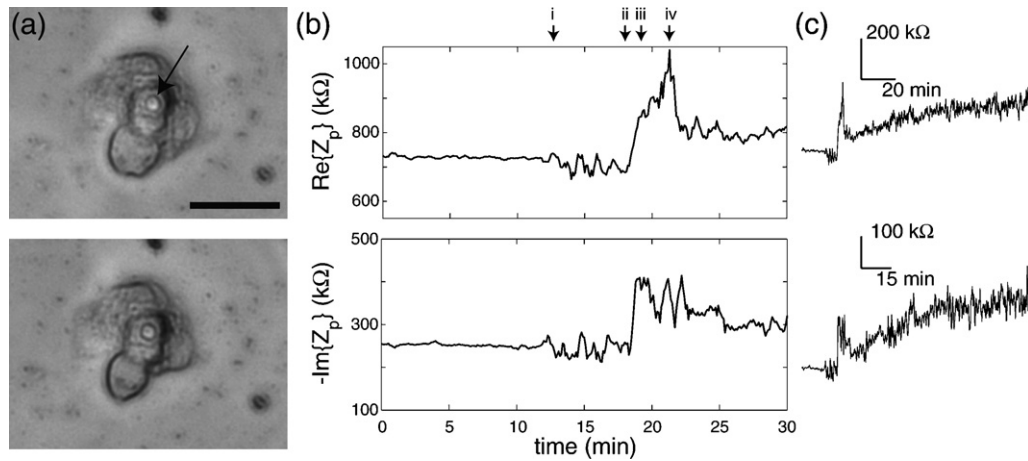


Fig. 5. (a) Macrophages held at a capture pore (arrow) at $t=0$ (top) and $t=120$ min (bottom). Scale bar = $20 \mu\text{m}$. (b) $Re\{Z_p(1000)\}$ and $Im\{Z_p(1000)\}$ of the capture pore for the first 30 min of an LPS challenge. Arrows show the infusion of LPS ($100 \mu\text{g/mL}$) (i), a rise in $Re\{Z_p\}$ (ii), a second, less steep rise (iii), and a reduction in $Re\{Z_p\}$ (iv). (c) $Re\{Z_p(1000)\}$ and $Im\{Z_p(1000)\}$ for the full time-course (120 min) of LPS challenge.

ing (Schmidt et al., 2001). Cho et al. predicted and demonstrated the electrical detection of increased attachment and spreading of cells held at a micro-hole (Cho and Thielecke, 2007). This group predicted two responses of a cell located at a micro-hole that would lead to an increase in detected resistance across the micro-hole: (1) increased spreading would increase the path-length over which ions must flow and (2) increased adhesion would reduce the gap between the cell and the chip and thus reduce the cross-sectional area over which ions must flow. Here, our objective is to determine if LPS-induced spreading and adhesion of macrophages can be detected electrically at the level of single cells.

For an immune challenge experiment, the same procedure for capturing a cell as described in Section 3.1.1 was followed. All media were pre-warmed to 37°C , and the device assembly was fully encapsulated except for a single capillary outlet emptying to a waste beaker. For injecting the immune challenge (LPS) into the top chamber, a second three-way valve was coupled to the top chamber outlet capillary that normally empties into a waste reservoir. LPS-containing medium is then injected through the top outlet, and the waste medium from the chamber exits what was previously the top inlet. This procedure eliminates the possibility of exposing cells to the chal-

lenge prior to capture at the pore in the top chamber. Fig. 5 shows a macrophage held at a capture pore surrounded by several additional macrophages that have landed and attached adjacent to the captured cell. Growth medium was perfused into the top chamber during the first 12 min of the experiment, and the average impedance across the pore at 1 kHz was $Re\{Z_p\} = 730 \pm 7 \text{ k}\Omega$ and $Im\{Z_p\} = -250 \pm 6 \text{ k}\Omega$. LPS ($100 \mu\text{g/mL}$) was then perfused into the chamber at a flow rate of $100 \mu\text{L/min}$ (Fig. 5b, arrow i). At this rate, the top chamber will fill with LPS in ~ 2 min. After the LPS reached the chamber, the flow rate was lowered to $20 \mu\text{L/min}$. The average impedance across the pore slightly dropped to $Re\{Z_p\} = 700 \pm 46 \text{ k}\Omega$ and $Im\{Z_p\} = -240 \pm 43 \text{ k}\Omega$ for the next 6 min (from 12 to 18 min), largely due to the higher conductivity of the LPS-containing growth medium. At 18 min into the experiment, there is a rapid increase in $Re\{Z_p\}$ across the pore (Fig. 5b, arrow ii), then a period of slower increase for 2 min (Fig. 5b, arrow iii), and then a rapid decline (Fig. 5, arrow iv). At $t=27$ min, $Re\{Z_p\}$ begins to rise slowly, continuing throughout the rest of the 2 h experiment (Fig. 5c, top). The final pore impedance magnitude and phase (averaged over the last 40 min) increased to $Re\{Z_p\} = 930 \pm 58 \text{ k}\Omega$ and $Im\{Z_p\} = -440 \pm 60 \text{ k}\Omega$. The cause of these changes in impedance during the time-course of this

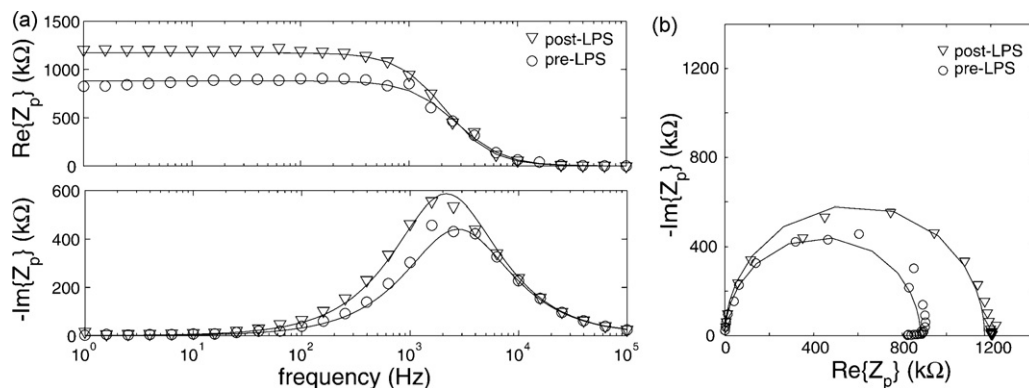


Fig. 6. (a) $Re\{Z_p\}$ and $Im\{Z_p\}$ of a captured macrophage before exposure to LPS and at the end of the LPS challenge. Solid lines are RC element fits to the experimental data. (b) Complex plane impedance plot of the pre- and post-LPS impedance data.

experiment is unknown. They could be an indication of dynamic changes in cell-substrate coupling as time-lapse imaging has shown these cells to be motile when attached to substrates (data not shown). Fig. 6 shows the frequency spectrum of the captured macrophage before LPS challenge and after the 2 h challenge experiment. Prior to LPS exposure, the frequency spectrum of the macrophage is fit by $R_p = 881.3 \text{ k}\Omega$ and $C_p = 65.2 \text{ pF}$ ($r^2 = 0.9977$), and after the LPS challenge, the impedance spectrum is fit by $R_p = 1.2 \text{ M}\Omega$ and $C_p = 63.1 \text{ pF}$ ($r^2 = 0.9953$). After the impedance analysis was complete, the cell was removed from the capture pore with positive pressure.

4. Conclusions

We have used the previously described cell capture chip and electrofluidic assembly to demonstrate non-invasive reversible impedimetric measurements of single macrophages. The parylene coating improves the impedimetric characteristics of the chip, and also provides a reversible and gentle mechanical coupling between the cell and the chip. Cells are captured under negative pressure, assessed for viability, and then subjected to long-term chemical challenges. Cells are first rapidly and non-invasively assessed for viability by examining the low-frequency value of $Re\{Z_p\}$ and mid-frequency value of $Im\{Z_p\}$, allowing only cells that meet a user-defined threshold to continue with a chemical challenge and further analysis. Here, we assessed the response of macrophages to an immune stimulant, and observed an increase in the impedance across the capture pore holding the cell. This is likely due to an increase in adherence/spreading of the cell after LPS stimulation. Measurements on macrophages using electrical impedance (Kowolenko et al., 1990) and quantitative image analysis (Schmidt et al., 2001) showed similar increases in cell spreading/adherence after LPS stimulation. Simulations performed by Cho et al. also predict a rise in impedance across a cell held at a micro-hole that undergoes increased spreading or adhesion (Cho and Thielecke, 2007). Further experiments with 3D confocal imaging are required to investigate the correlation between impedance measurements and morphological changes in cells adhered to substrates.

Acknowledgements

We would like to thank the Microelectronics Development Laboratory staff and management at Sandia National Laboratories for device fabrication. We also extend our gratitude to Jaime McClain and Patricia Sawyer for cell and device preparation, as well as experimental support, and Craig Nakakura and Mark Jenkins for AFM and SEM imaging, respectively. This work was performed as part of the Microscale Immune Studies Laboratory Grand Challenge project funded by Sandia's Laboratory Directed Research and Development program. Sandia is

a multiprogram laboratory operated by Sandia Corporation, a Lockheed Martin Company, for the United States Department of Energy under contract DE-AC04-94AL85000.

Appendix A. Supplementary data

Supplementary data associated with this article can be found, in the online version, at doi:10.1016/j.bios.2007.08.022.

References

- Cho, S., Thielecke, H., 2007. *Biosens. Bioelectron.* 22, 1764–1768.
- Davidsson, R., Boketoft, A., Bristulf, J., Kotarsky, K., Olde, B., Owman, C., Bengtsson, M., Laurell, T., Emneus, J., 2004. *Anal. Chem.* 76, 4715–4720.
- Di Carlo, D., Lee, L.P., 2006. *Anal. Chem.* 78, 7918–7925.
- Di Carlo, D., Ionescu-Zanetti, C., Zhang, Y., Hung, P., Lee, L.P., 2005. *Lab Chip* 5, 171–178.
- Feili, D., Schuettler, M., Doerge, D., Kammer, S., Stieglitz, T., 2005. *Sens. Actuators A* 120, 101–109.
- Fertig, N., Blick, R.H., Behrends, J.C., 2002. *Biophys. J.* 82, 3056–3062.
- Giaever, I., Keese, C.R., 1991. *Proc. Natl. Acad. Sci. U.S.A.* 88, 7896–7900.
- Han, A., Frazier, A.B., 2006. *Lab Chip* 6, 1412–1414.
- Huang, Y., Rubinsky, B., 2001. *Sens. Actuators A* 89, 242–249.
- Huang, Y., Sekhon, N.S., Borninski, J., Chen, N., Rubinsky, B., 2003. *Sens. Actuators A* 105, 31–39.
- Keese, C.R., Giaever, I., 1994. *IEEE Eng. Med. Biol. Mag.* 13, 402–408.
- Khine, M., Lau, A., Ionescu-Zanetti, C., Seo, J., Lee, L.P., 2005. *Lab Chip* 5, 38–43.
- Klemic, K.G., Klemic, J.F., Sigworth, F.J., 2005. *Pflugers Arch.-Eur. J. Physiol.* 449, 564–572.
- Kowolenko, M., Keese, C.R., Lawrence, D.A., Giaever, I., 1990. *J. Immunol. Methods* 127, 71–77.
- Lee, J., Cheong, K.H., Huh, N., Kim, S., Choi, J., Ko, C., 2006a. *Lab Chip* 6, 886–895.
- Lee, E.S., Robinson, D., Rognlien, J.L., Harnett, C.K., Simmons, B.A., Ellis, C.R.B., Davalos, R.V., 2006b. *Bioelectrochemistry* 69, 117–125.
- Li, N., Tourovskaia, A., Folch, A., 2003. *Crit. Rev. Biomed. Eng.* 31, 423–488.
- Lidstrom, M.E., Meldrum, D.R., 2003. *Nat. Rev. Microbiol.* 1, 158–164.
- Longo, D., Hasty, J., 2006. *Mol. Syst. Biol.* 2, 1–10.
- Matthews, B., Judy, J.W., 2006. *J. Microelectromech. Syst.* 15, 214–222.
- Morland, B., Kaplan, G., 1977. *Exp. Cell Res.* 108, 279–288.
- Munoz-Pinedo, C., Green, D.R., van den Berg, A., 2005. *Lab Chip* 5, 628–633.
- Pantoja, R., Nagaraj, J.M., Starace, D.M., Melosh, N.A., Blunck, R., Bezanilla, F., Heath, J.R., 2004. *Biosens. Bioelectron.* 20, 509–517.
- Rabinovitch, M., Destefano, M.J., 1974. *Exp. Cell Res.* 88, 153–162.
- Schmidt, A., Caron, E., Hall, A., 2001. *Mol. Cell. Biol.* 21 (2), 438–448.
- Shackman, J.G., Dahlgren, G.M., Peters, J.L., Kennedy, R.T., 2005. *Lab Chip* 5, 56–63.
- Suzuki, H., Tabata, K., Kato-Yamada, Y., Noji, H., Takeuchi, S., 2004. *Lab Chip* 4, 502–505.
- Thompson, D.M., King, K.R., Wieder, K.J., Toner, M., Yarmush, M.L., Jayaraman, A., 2004. *Anal. Chem.* 76, 4098–4103.
- Valero, A., Merino, F., Wolbers, F., Lutge, R., Vermes, I., Andersson, H., van den Berg, A., 2005. *Lab Chip* 5, 49–55.
- Walker, G.M., Zeringue, H.C., Beebe, D.J., 2004. *Lab Chip* 4, 91–97.
- Wegener, J., Keese, C.R., Giaever, I., 2000. *Exp. Cell Res.* 259, 158–166.
- Whitesides, G.M., Ostuni, E., Takayama, S., Jiang, X., Ingber, D.E., 2001. *Ann. Rev. Biomed. Eng.* 3, 335–373.
- Wieder, K.J., King, K.R., Thompson, D., Zia, C., Yarmush, M.L., Jayaraman, A., 2005. *Biomed. Microdevices* 7, 213–222.